

# Self-directed growth of iron core–shell oval-shaped nanorods and nanocubes on a H-terminated Si(100) substrate in an external magnetic field

L Y Zhao, K R Eldridge, T Chan, N Panjwani and K T Leung<sup>1</sup>

Department of Chemistry, University of Waterloo, Waterloo, ON, N2L 3G1, Canada

E-mail: [tong@uwaterloo.ca](mailto:tong@uwaterloo.ca) (K T Leung)

Received 14 March 2007, in final form 11 April 2007

Published 25 May 2007

Online at [stacks.iop.org/Nano/18/245703](http://stacks.iop.org/Nano/18/245703)

## Abstract

Iron core–shell oval-shaped nanorods and nanocubes were electrodeposited on a H-terminated Si(100) substrate with and without the presence of an externally applied magnetic field (with a flux density of 1.3 T). The presence of an external magnetic field during electrodeposition was found to produce clustering of oval-shaped nanorods with short-range ordering in the long-axis orientation, and to induce self-assembly of nanocubes into stripes along the field-line direction. Glancing-incidence x-ray diffraction showed that the magnetic field also changed the distribution of the crystal orientations of the Fe nanocubes. An external magnetic field applied during electrodeposition could therefore be used to manipulate the spatial and crystallographic arrangements of the deposited Fe nanoparticles.

## 1. Introduction

Iron magnetic nanoparticles (NPs) have attracted a lot of recent attention because of their potential applications in magnetic recording media [1], targeted drug delivery [2], and spin-based electronics [3]. Unlike vacuum-based deposition techniques, electrodeposition is a simple and cost-effective method to synthesize Fe NPs on a substrate often at ambient temperature. These deposition techniques are also capable of producing interfaces appropriate for potential applications in microelectronics [4]. Although electrodeposition has been used extensively to produce a uniform, homogeneous Fe film on a chosen substrate [5], there is virtually no work reported for Fe NP growth on a substrate by electrochemistry. In the case of a magnetic material such as Fe, we have recently demonstrated that near-monosized and uniformly distributed oval-shaped nanorods (130 nm length  $\times$  25 nm diameter, and with a mixed FeOOH and FeO shell) [6] and nanocubes (with an average side-length of 56 nm and a predominant Fe core) [7] could be deposited electrochemically on a H-terminated Si(100) surface in FeCl<sub>3</sub> and FeCl<sub>2</sub> solutions, respectively. In the present work,

we demonstrate that an externally applied magnetic field can be used to guide the growth of these magnetic NPs during electrodeposition. Such two-dimensional spatial control of the deposited NPs is highly desirable for potential applications and development of nanoscale devices.

To date, magnetic-field-guided effects on magnetic NPs have not been reported. However, application of an external magnetic field has been known to play an important role for controlling electroplating of metallic Fe films. In particular, Yang reported that the presence of a magnetic field with a flux density  $B$  of 0.54 T during Fe electrodeposition had no significant effect on the crystal orientation of the deposited film [8]. However, the resulting surface morphology was found to be very rough and with protrusions in the direction of the magnetic field when applied perpendicular to the sample, in contrast to that found for the deposited surface obtained without a magnetic field and when the magnetic field was applied parallel to the surface. Li and Szpunar simulated the texture formation during Fe electrodeposition by using a Monte Carlo model [9, 10]. Consistent with their electrochemistry experiments, their simulations showed that under a sufficiently strong magnetic field parallel to the cathode surface, the as-formed fibre texture was gradually replaced by a non-fibre

<sup>1</sup> Author to whom any correspondence should be addressed.

texture due to the magnetocrystalline anisotropy. Bodea *et al* investigated the electrodeposition of Fe from a thin layer of aqueous  $\text{FeSO}_4$  solution under a magnetic field in the plane of the sample surface [11], and found that the macroscopic morphology of the Fe tree-like aggregates changed from circular to rectangular when deposited in the presence of a magnetic field. Kwon *et al* studied the effect of a magnetic field on Fe electrodeposition into the pores of an aluminium anodic oxide film [12]. The magnetic field was found to have little effect on the coercivity of the deposited Fe film without any preferred orientation of the Fe crystals. Matsushima *et al* examined Fe electrodeposition with a magnetic field with  $B = 0\text{--}5$  T parallel to the cathode surface [13]. At a current density of  $30\text{ mA cm}^{-2}$  or higher, the magnetic field was found to have no effect on the crystal orientation and texture. At a lower current density of  $10\text{ mA cm}^{-2}$ , the Fe current efficiency appeared to decrease with increasing magnetic flux. Although the crystal orientation was also not affected by the presence of a magnetic field, biaxial texture with roundish grains and smooth surface was found in the case of the magnetic field, in contrast to the uniaxial texture with angular grains and a large size distribution observed without the magnetic field. It should be noted that the (110) plane was determined to be in the same direction as the magnetic field at  $30^\circ$  with respect to the normal of the cathode plane. This result was contradictory to the previous result [9, 10], where the (100) plane was reported to be parallel to the magnetic field. In a following work, Matsushima *et al* [14] reported that at  $30\text{ mA cm}^{-2}$  the surface morphology changed from a triangular pyramid shape at no field to a star-like shape in a magnetic field with  $B = 5$  T parallel to the cathode surface. Contrary to their previous report [13], they found that the crystal texture could be controlled by the magnetic field, where the (110) plane was oriented in the same direction as the magnetic field at  $35^\circ$  from the normal of the cathode plane. They further reported that the surface morphology of the Fe film was roundish and uniform with the magnetic field perpendicular to the cathode surface, while the Fe grains became undulative when the magnetic field was parallel to the cathode surface [15, 16]. These studies therefore illustrate the complex effects that an externally applied magnetic field could produce on the macroscopic and microscopic properties of the deposited Fe films.

To date, no study on the effect of magnetic field on the electrodeposition of metallic Fe NPs has been reported. In the present work, we report the first result demonstrating the effects of an external magnetic field on the electrodeposition of Fe NPs, which suggests that an external magnetic field could be used to manipulate the NP growth, particularly to induce self-assembly, on a Si substrate.

## 2. Experimental details

The electrodeposition experiments were performed in a three-electrode cell with a potentiostat/galvanostat electrochemical workstation. Details of our three-electrode cell set-up and the electrodeposition experiments have been described elsewhere [6]. Our Si(100) substrates (p-type,  $30 \times 15\text{ mm}^2$ , 0.4 mm thick,  $1.0\text{--}1.5\text{ m}\Omega\text{ cm}$ ) were cleaned by using the RCA method, etched in aqueous HF (2%) solution to remove the

native oxide layer, and rinsed with Millipore water [17]. The resulting H-Si(100) (i.e. H-terminated) is atomically flat and mainly terminated with dihydride, which has been found to be suitable for uniform deposition of nanoparticles<sup>2</sup>. For the oval-shaped nanorods [6], the electrodeposition was conducted in a deoxygenated aqueous solution of 10 mM  $\text{FeCl}_3$  and 0.1 M  $\text{NaClO}_4$  (at  $-0.8$  V for 1 s). For the nanocubes [7], a deoxygenated aqueous solution of 10 mM  $\text{FeCl}_2$  and 0.2 M  $\text{H}_3\text{BO}_3$  was used for the electrodeposition (at  $-1.4$  V for 5 s). It should be noted that the oval shape of the nanorods could be caused by codeposition with  $\text{FeOOH}$  formed by hydrolysis in the aqueous  $\text{FeCl}_3$  solution. Since hydrolysis could not occur in an  $\text{FeCl}_2$  solution and well-defined Fe NPs are probably single crystalline (bcc), the deposited Fe NPs therefore have the expected cubic shape.

A 5 mm thick rectangular neodymium magnet ( $25 \times 10\text{ mm}^2$ ) with  $B = 1.3$  T was used to generate the external magnetic field. The magnet was carefully placed parallel and as close to the backside of the Si substrate as possible (without physical contact), and the angle between the magnetic field and the electric field for the electrodeposition was  $60^\circ$ . The surface morphology of the Fe NPs resulting from the magnetic-field-guided electrodeposition was characterized by field-emission scanning electron microscopy (SEM). The structures of the nanodeposits were further determined by glancing-incidence x-ray diffraction (GIXRD), with an incidence angle  $\omega$  of  $0.6^\circ$  and the Cu  $K\alpha$  anode operating at 45 kV and 40 mA. The divergent x-ray beam was collimated by a graded multilayer parabolic x-ray mirror, and the x-ray spot size on the sample surface was further defined by a 10 mm beam mask and a  $1/16^\circ$  divergence slit.

## 3. Results and discussion

Figure 1 compares the surface morphologies of the Fe oval-shaped nanorods obtained with and without the presence of an external magnetic field. In the absence of an externally applied magnetic field (figures 1(a) and (b)), the nanorods appear to be uniformly distributed on the Si substrate. There is also no apparent short-range ordering in the orientation of these oval-shaped nanorods and the nanorods appear to be randomly distributed. In the presence of the magnetic field, self-assembly of the Fe nanorods is clearly evident (figures 1(c) and (d)). The nanorods appear to cluster together, creating regions of high and low number densities (figures 1(c)). In regions of high number densities (figure 1(d)), short arrays of the oval-shaped nanorods with individual long-axes aligned near-parallel to one another are seen, which indicates limited short-range ordering of the NP deposition. In regions of low number densities, no short-range ordering is observed (figure 1(c)). A similar observation can be made for the deposited Fe nanocubes obtained with and without the presence of an external magnetic field, as shown in figure 2. Evidently, self-assembly of these NPs into 'stripes' of nanocubes is obtained by electrodeposition in the presence of the magnetic field (figures 2(c) and (d)), in sharp contrast to the homogeneous deposition observed in the absence of the magnetic field

<sup>2</sup> It should be noted that electrodeposition typically produces surface silicon suboxide ( $\text{SiO}_x$ ) due to partial oxidation of the Si substrate in an aqueous solution, as confirmed by XPS analysis.

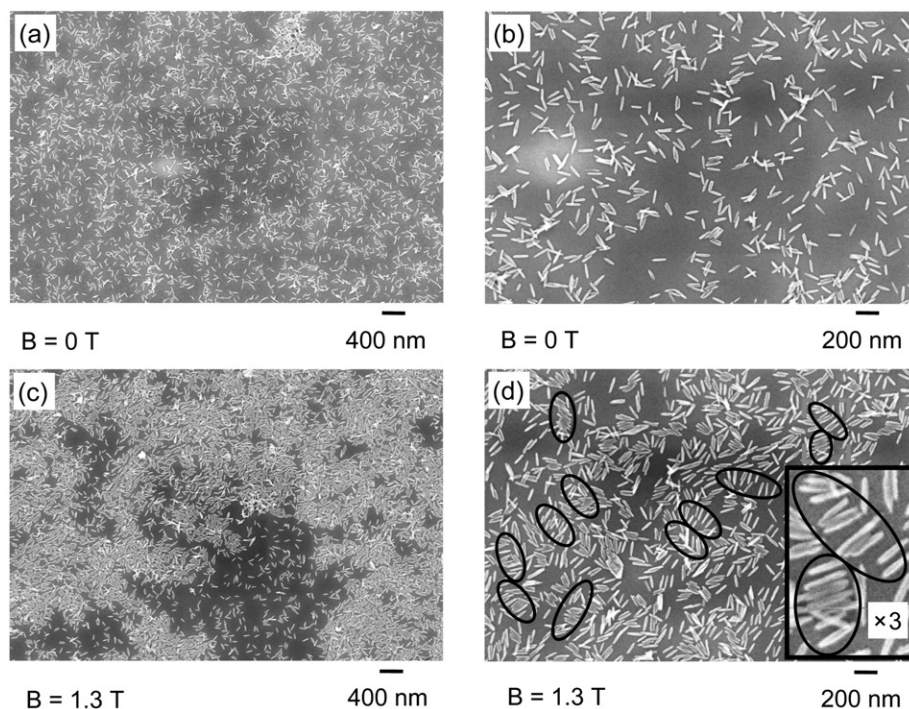


**Figure 1.** SEM images of Fe oval-shaped nanorods electrodeposited on H-Si(100) in an aqueous solution of 10 mM  $\text{FeCl}_3$  and 0.1 M  $\text{NaClO}_4$  at  $-0.8$  V for 1 s without ((a), (b)) and with ((c), (d)) the presence of external magnetic field (with flux density  $B = 1.3$  T). A magnified view of a highlighted region illustrating short-range alignment of the nanorods is shown as inset in (d).

(figures 2(a) and (b)). When the separation between the neodymium magnet and the Si substrate is increased to  $>1$  mm, no stripe is observed. Our present set-up limited our experiment to the angle between the magnetic field and electric field fixed at  $60^\circ$ . It should be very interesting to investigate any effects on the NP morphology as a result of different orientations of magnetic field relative to the electric field. The number density of the NPs in the stripe region ( $3.23 \times 10^9 \text{ cm}^{-2}$ , figure 2(e)) is found to be discernibly higher than that in the other regions ( $2.93 \times 10^9 \text{ cm}^{-2}$ , figure 2(f)). In the stripe region, codeposition of feather-like structures is also observed along with the cuboidal NPs, which could be due to the accelerated growth rate of the Fe electrodeposition mediated by the magnetic field.

The electrodeposition for both the oval-shaped nanorods and nanocubes in the presence of a magnetic field clearly shows that nucleation is concentrated by or along the direction of the magnetic field lines. A possible explanation is that upon reduction of  $\text{Fe}^{3+}$  or  $\text{Fe}^{2+}$  to metallic  $\text{Fe}^0$ , the deposited  $\text{Fe}^0$  atoms, being ferromagnetic, become magnetized by the external magnetic field. The nucleated Fe clusters (as the seeds for the NP growth) could in turn induce magnetization of the incoming  $\text{Fe}^{3+}$  or  $\text{Fe}^{2+}$  ions, producing dipolar interactions to attract the paramagnetic ions to further deposit in or near the nucleation sites. Electrodeposition of the  $\text{Fe}^{2+}$  ions has been shown to produce a dominant Fe core before the formation of the oxide shell [7], which generates a strong magnetization effect and therefore the observed self-assembled stripes of nanocubes (figure 2(d)). For electrodeposition involving  $\text{Fe}^{3+}$  ions, however, the amount of Fe core was found to be limited and the oval-shape of the nanorod nanostructure could be due

to codeposition of  $\text{FeOOH}$  during electrodeposition of the Fe NPs [6]. The formation of the  $\text{FeOOH}$  shell becomes prominent once a critical core dimension has been reached. The relatively small amount of Fe core in the resulting oval-shaped nanorod is apparently insufficient to generate the large magnetization effect as observed in the  $\text{Fe}^{2+}$  case. Only clustering or grouping of NP growth is observed. Due to the close spacing of these nucleated sites and the inter-particle magnetic interaction of the NPs, the uniformly sized antiferromagnetic  $\text{FeOOH}$  shells covering the Fe cores are seen with the long axes of the nanorods partially aligned with a limited ordering. This phenomenon is illustrated by the (highlighted) rows of 7–13 oval-shaped NPs all aligned parallel to one another in figure 1(d).

When a magnetic field was applied perpendicular to the electric field during the electrodeposition, the magnetic field could induce convection due to the Lorentz force and consequently affect the migration of ions. This so-called magnetohydrodynamic (MHD) effect is often used to explain the magnetic-field-induced changes to the electrodeposition of thin films. In the earlier work involving Fe film electrodeposition in the presence of an external magnetic field, the current density used was  $10\text{--}30 \text{ mA cm}^{-2}$  [13]. However, the current densities ( $3 \text{ mA cm}^{-2}$  for Fe nanorods and  $7 \text{ mA cm}^{-2}$  for Fe nanocubes) used in the present work are considerably lower. We therefore expect that the MHD effect would not play a prominent role in the present case, and the influence of magnetic field on NP growth becomes more apparent due to the weaker electric field. Furthermore, the MHD effect is found to be the strongest when mass transport is the controlling factor for the metal deposition

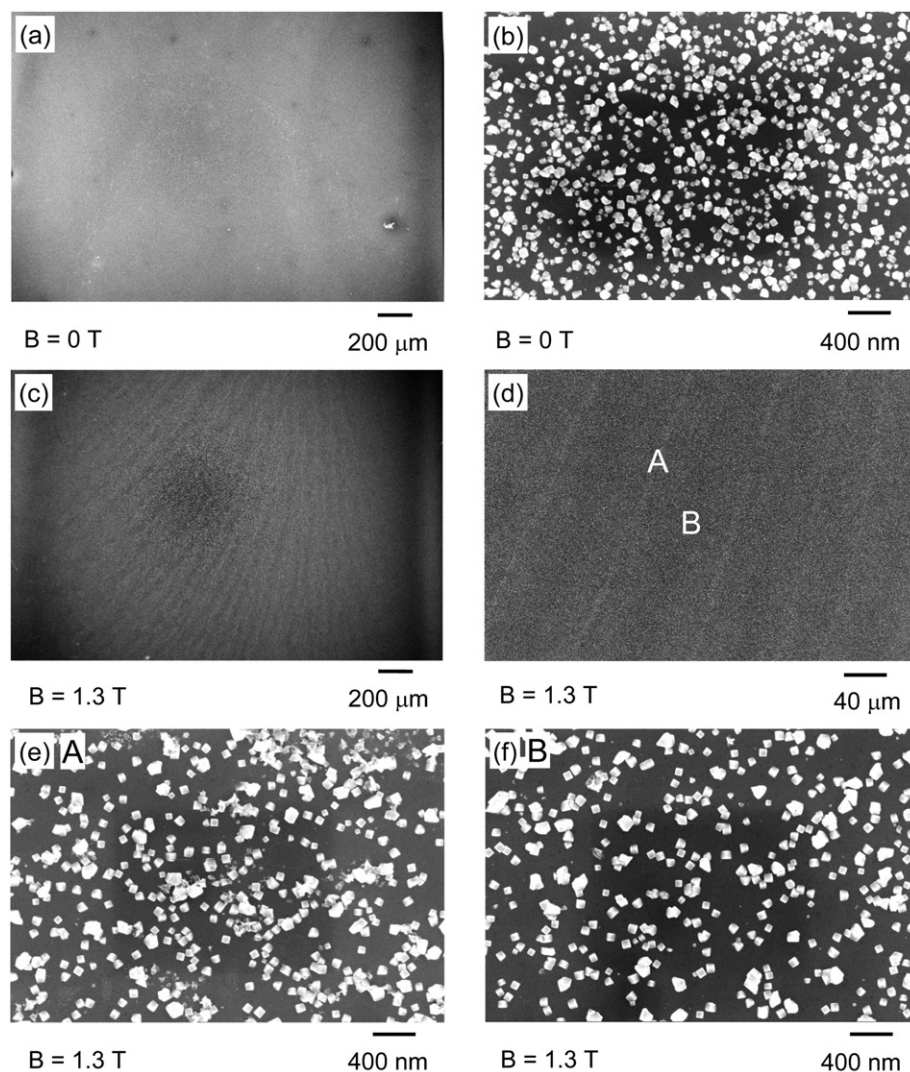


**Figure 2.** SEM images of Fe nanocubes electrodeposited on H-Si(100) in an aqueous solution of 10 mM  $\text{FeCl}_2$  and 0.2 M  $\text{H}_3\text{BO}_3$  at  $-1.4$  V for 5 s without ((a), (b)) and with ((c)–(f)) the presence of magnetic field with flux density  $B = 1.3$  T; (e) and (f) are taken at a higher magnification at points A (stripe region) and B (in-between stripes) in (d).

(where bulk convection and narrowing of the diffusion layer on the working electrode surface would occur) [18]. In the case of Fe electrodeposition that is largely controlled by charge transfer [14], the MHD effect is found to be weak. If the MHD effect is present, bulk convection would be induced and narrowing of the diffusion layer on the working electrode surface would occur (in the presence of a magnetic field), which would in turn increase the current density. The lack of change in the current density for NP electrodeposition with and without the presence of an external magnetic field as observed in the present work is therefore consistent with negligible MHD effect. We therefore conclude that the MHD effect can be neglected in the present consideration of the underlying magnetic-field-guided mechanism.

In addition to the morphological changes in the magnetic-field-guided electrodeposition, we also observe changes to the crystallographic orientation in the Fe cubic NPs. Figure 3 compares the GIXRD patterns of the Fe nanocubes deposited on H-Si(100) substrate with and without the presence of the

external magnetic field. The features at  $50^\circ$ – $60^\circ$  are found to be in good accord with the (311) plane of the p-Si(100) substrate reported in the literature [19]. All of the remaining peaks found for the Fe NPs shown in figure 3 can be assigned to the (110), (200), (211), (220) and (310) planes of the body-centred cubic (bcc) lattice of Fe (JCPDS 06-0696). Evidently, the (310) intensity is found to be discernibly smaller in the case of the magnetic-field-guided deposition, and this change can be quantified by the crystallographic orientation index  $M(hkl)$  as described in the literature [20]. In particular, the  $M(110)$ ,  $M(200)$ ,  $M(211)$ ,  $M(220)$  and  $M(310)$  are estimated to be 1.2, 0.6, 0.7, 0.8 and 1.0, respectively, for the case without the external magnetic field (figure 3(a)). The  $M(310)$  value (0.7) is found to decrease (while the others remain unchanged) in the presence of the magnetic field (figure 3(b)). The external magnetic field could therefore produce notable changes to the relative distribution of the NPs with different orientations, i.e., reduction in the relative populations of cubic NPs with the (310) plane orientation. It should be noted that for the Fe oval-

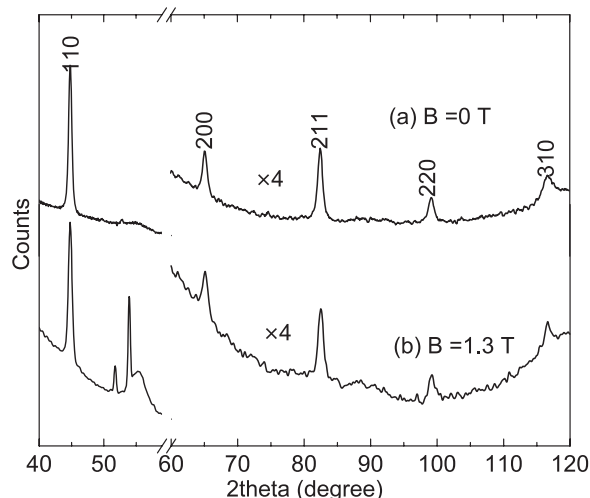


**Figure 3.** Glancing-incidence XRD patterns of Fe nanocubes electrodeposited on H-Si(100) in an aqueous solution of 10 mM FeCl<sub>2</sub> and 0.2 M H<sub>3</sub>BO<sub>3</sub> at -1.4 V for 5 s (a) without and (b) with the presence of an external magnetic field with flux density  $B = 1.3$  T.

shaped nanorods, the corresponding GIXRD spectrum (not shown) was found to exhibit the same features as FeOOH, indicating that the amount of Fe core was just too small to produce a detectable GIXRD pattern.

#### 4. Concluding remarks

The application of an external magnetic field during electrodeposition has been shown to produce dramatic changes in the morphology and crystallographic distribution of Fe NP growth on a H-Si(100) substrate. In particular, self-assembly of Fe oval-shaped nanorods with apparent short-range ordering along the long-axis direction and of nanocubes into stripes along the magnetic-field-line direction are found for deposition involving, respectively, Fe<sup>3+</sup> and Fe<sup>2+</sup> electrolytes in the presence of an external magnetic field. In marked contrast to the earlier studies on Fe film electrodeposition that show that an external magnetic field does not produce any observable changes in the crystal orientation, the present work illustrates for the first time that the relative populations of certain crystal orientations in the Fe nanocube growth can be changed by the

external magnetic field. The present result therefore suggests that application of an external magnetic field could be used not only to induce self-assembly and spatial alignment of the NPs during growth but also to manipulate the nanocrystal growth with preferred crystallographic orientation.

#### Acknowledgment

This work was supported by the Natural Sciences and Engineering Research Council of Canada.

#### References

- [1] Sun S, Murray C B, Weller D, Folks L and Moser A 2000 *Science* **287** 1989
- [2] Tartaj P, Morales M P, Veintemillas-Verdaguer S, González-Carreño T and Serna C J 2003 *J. Phys. D: Appl. Phys.* **36** R182
- [3] Bobo J F, Gabillet L and Bibes M 2004 *J. Phys.: Condens. Matter* **16** S471
- [4] Murarka S P 1983 *Silicides for VLSI Applications* (New York: Academic)
- [5] Schlesinger M and Paunovic M 2000 *Modern Electroplating* 4th edn (New York: Wiley) p 461
- [6] Zhao L Y, Eldridge K R, Sukhija K, Jalili H, Heinig N F and Leung K T 2006 *Appl. Phys. Lett.* **88** 033111
- [7] Zhao L Y, Jalili H, Panjwani N, Chan T, Heinig N F and Leung K T 2007 to be submitted
- [8] Yang L 1954 *J. Electrochem. Soc.* **101** 456
- [9] Li D Y and Szpunar J A 1997 *Electrochim. Acta* **42** 37
- [10] Li D Y and Szpunar J A 1997 *Electrochim. Acta* **42** 47
- [11] Bodea S, Vignon L, Ballou R and Molho P 1999 *Phys. Rev. Lett.* **83** 2612
- [12] Kwon H W, Kim S K and Jeong Y 2000 *J. Appl. Phys.* **87** 6185
- [13] Matsushima H, Nohira T, Mogi I and Ito Y 2004 *Surf. Coat. Technol.* **179** 245
- [14] Matsushima H, Nohira T and Ito Y 2004 *J. Solid State Electrochem.* **8** 195
- [15] Matsushima H, Nohira T and Ito Y 2004 *Electrochem. Solid State Lett.* **7** C81
- [16] Matsushima H, Fukunaka Y, Ito Y, Bund A and Plieth W 2006 *J. Electroanal. Chem.* **587** 93
- [17] Kern W (ed) 1993 *Handbook of Semiconductor Wafer Cleaning Technology* (Park Ridge: Noyes)
- [18] Fahidy T Z 1983 *J. Appl. Electrochem.* **13** 553
- [19] Cho B O, Chang J P, Min J H, Moon S H, Kim Y W and Levin I 2003 *J. Appl. Phys.* **93** 745
- [20] Yoshimura S, Yoshihara S, Shirakashi T and Sato E 1994 *Electrochim. Acta* **39** 589